13th World Conference on Earthquake Engineering
Vancouver, B.C., Canada
August 1-6, 2004
Paper No. 196

DYNAMIC BEHAVIOR OF AN EIGHT-STOREY SRC BUILDING EXAMINED FROM STRONG MOTION RECORDS

Toshihide KASHIMA[1]

SUMMARY

A detailed strong motion observation is being conducted in buildings and in the surrounding grounds at Building Research Institute (BRI), Tsukuba, Japan. A number of acceleration sensors are configured in order to grasp complicated behavior of buildings and grounds during earthquakes. This report introduces the recording system and observation results. We also discuss dynamic characteristics of the building and effect of the surface geology by means of analyses of strong motion records.

More than 200 earthquake records have been obtained in the past several years. 113 records are selected in consideration of seismic intensities. Although the amplitude levels are not high, the records have adequate quality for the analyses.

First, amplification effects of the surface soil layers are investigated. Rational results can be obtained from the analysis using acceleration records from borehole sensors. Second, dynamic characteristics of the eight-storey building are discussed. Natural frequencies including torsional one can be detected through the spectral analysis. Finally, soil-structure interaction phenomena are examined. Contributions of swaying and rocking of the foundation to the building response are estimated.

INTRODUCTION

Building Research Institute (BRI), Japan, started the strong motion observation project in 1957. The observation network has been improved and enlarged in the past half century. BRI is now operating more than 70 strong motion stations for the purpose of contributing to the advance of the seismic design technology for buildings.

In 1998, BRI has installed the up-to-date strong motion equipment to an 8-storey steel reinforced concrete (SRC) building in BRI [1, 2]. Totally 22 acceleration sensors were placed in two buildings and the surrounding ground. We hope the recording system of this kind will be useful for discussing amplification effect of surface geology, phenomena of soil-structure interaction and dynamic behavior of buildings. This paper is introducing the recording system that is installed to buildings and in the ground at BRI and some observation results.

[1] Senior Research Engineer, Building Research Institute, Tsukuba, Japan, Email: kashima@kenken.go.jp

OUTLINE OF STRONG MOTION OBSERVATION

Geological conditions

BRI is located approximately 60 kilometers to the northeast from Tokyo. The site is situated on the diluvial heights between the Sakuragawa River flowing into the Kasumigaura Lake and the Kokaigawa River, a branch flow in the greater Tonegawa River water system.

Table 1 indicates the surface soil structure at BRI. The surface soil layers mainly consist of clay and fine sand. Rock layers cannot be found down to 90 meters under the ground. However we confirmed a gravel layer, which is relatively hard, at 88 meters in depth. Transfer functions of shear waves between ground surface and gravel layers at depths of 42 meters, 68 meters and 88 meters are shown in Figure 1. We assume here that damping ratios of the soil layers are 5% to 10 % according to soil types. The figure shows common predominant frequencies of 2 to 4 Hz and 9 Hz. Moreover, the transfer function of 88-meter layers has the peak at 1 Hz.

Table 1 Structure of surface soil layers

No.	H (m)	D (m)	V_P (m/s)	V_S (m/s)	ρ (t/m^3)	Soil Type
1	2.0	2.0	170	110	1.30	Loam
2	6.0	8.0	1430	200	1.30	Sandy Clay & Clayey Sand
3	6.0	14.0		160	1.50	Sandy Clay & Clay
4	8.0	22.0	1630	260	1.80	Fire Sand & Clayey Fine Sand
5	6.0	28.0	1500	200	1.75	Sandy Clay & Clay
6	14.0	42.0	1570	270		
7	6.0	48.0	1880	460	1.90	Gravel
8	8.0	56.0	1780	340	1.75	Sandy Clay & Clay
9	12.0	68.0	1690	290		
10	12.0	80.0	1790	380	1.95	Gravel & Fine Sand
11	8.0	88.0	1600	280	1.75	Sandy Clay & Clay
12				500	2.00	Gravel

H: Thickness, D: Depth, V_P: P-wave velocity, V_S: S-wave velocity, ρ: Density

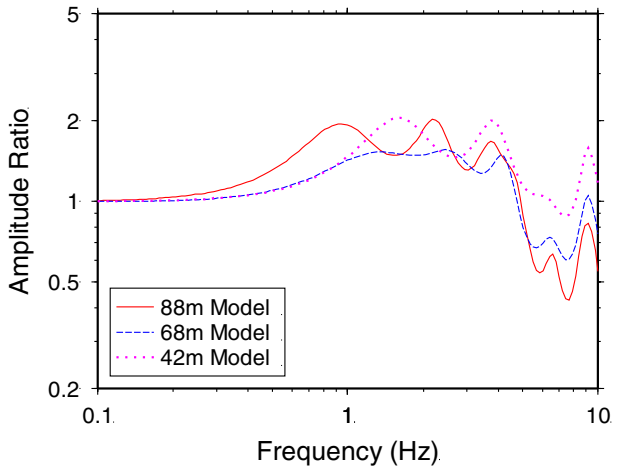

Figure 1 Transfer function of surface soil layers (A01/incidence)

Recording system

The strong motion recording system has eleven sensors (33 channels) in the annex building, seven sensors (21 channels) in the surrounding ground, and four sensors (12 channels) in the main building. The annex

building is a steel reinforced concrete building with eight storeys above ground and one below, and was completed in 1998. The amount of floor space is approximately 5,000 m^2 and the building is supported by the mat foundation on the clayey layer at 8.2 meters underground. The sensor configuration in the annex building is shown in Figures 2 and 3. The farthest sensor on the ground is placed 100 meters away from the annex building, and the deepest sensor is set up 89 meters in depth. Three sensors are installed at the basement floor and at the eighth floor in order to investigate torsional vibration.

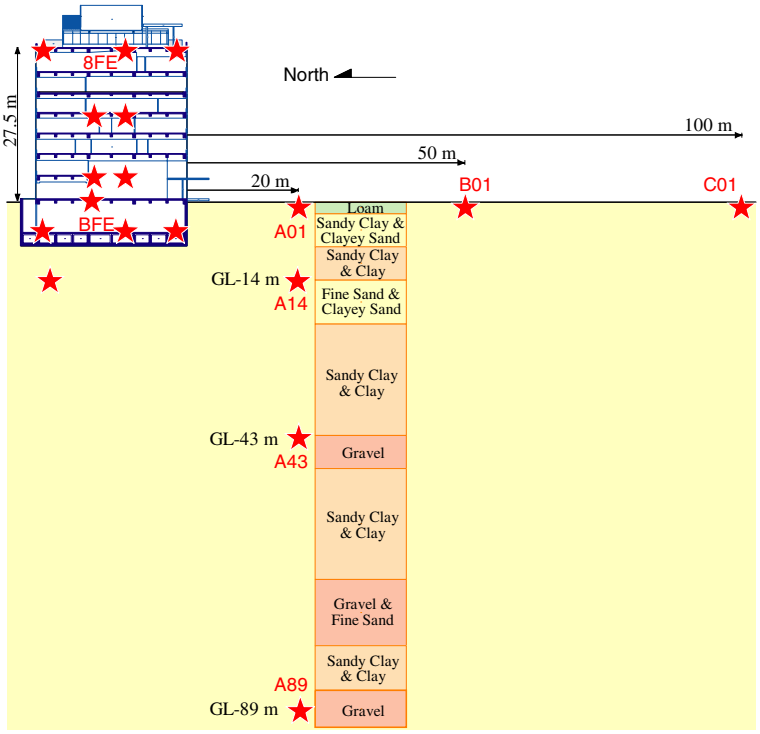

Figure 2 Vertical sensor configuration

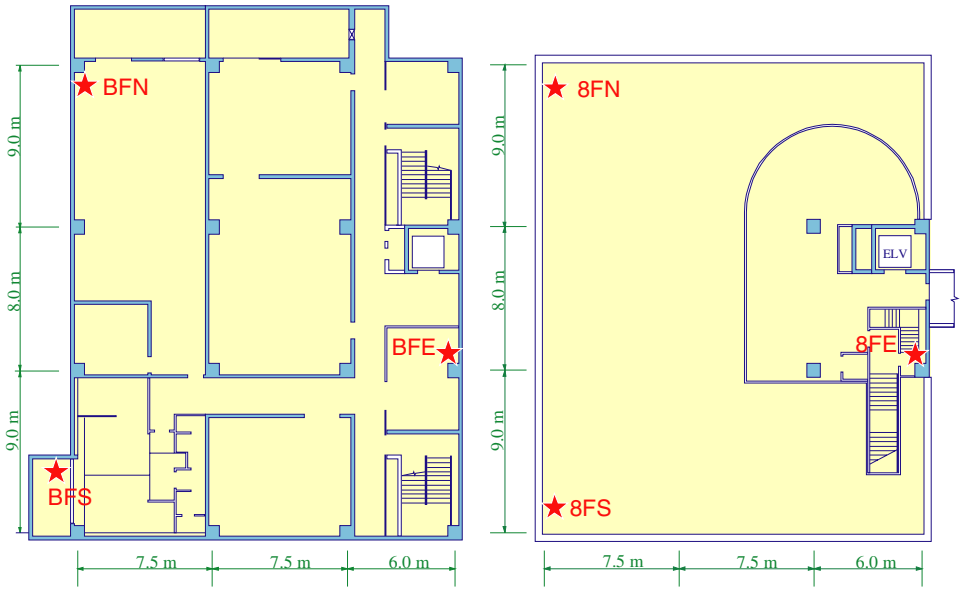

Figure 3 Sensor configurations at basement floor (left) and 8th floor (right)

All sensors are connected to the recording equipment at the observation room in the annex building. The specifications of the recording system are shown in Table 2. The system has 66-channel 24-bit A-D converters and a digital processing unit. PC cards are used as storage device and can be directly processed by PCs. Broad dynamic range and certain operation is ensured by the up-to-date facilities. The recording system is triggered if one of three components of the sensor at 89 meters below the ground feels more than 1 cm/s^2.

Table 2 Specifications of recording system

Model	AJE-8200, Akashi Corp.
Sensor	V403BT (negative feedback servo), Akashi Corp.
Number of Channels	66
Frequency Range	DC ~ 30 Hz
Acceleration Range	± 2 G
A/D Converter	24-bit (Delta-Sigma)
Dynamic Range	114 dB
Recording Medium	ATA Flash Memory Card
Triggering Logic	Disjunction (OR) of Specified Three Channels (1cm/s^2 at A89)
Functions	Peaks, JMA Seismic Intensity, Spectral Intensity (SI)

Observed records

In the past several years, we have obtained more than 200 earthquake records from this system. In consideration of seismic intensities at the site, 113 records are selected for the following analysis. The relation between epicentral distances and peak accelerations on the ground (A01) of those earthquakes is shown in Figure 4. Size and colour of symbols in the figure represent magnitudes of earthquakes determined by Japan Meteorological Agency (JMA). We have only records with moderate or small amplitudes. The largest peak ground acceleration was 74 cm/s^2. Therefore the following discussion cannot deal with non-linear problem.

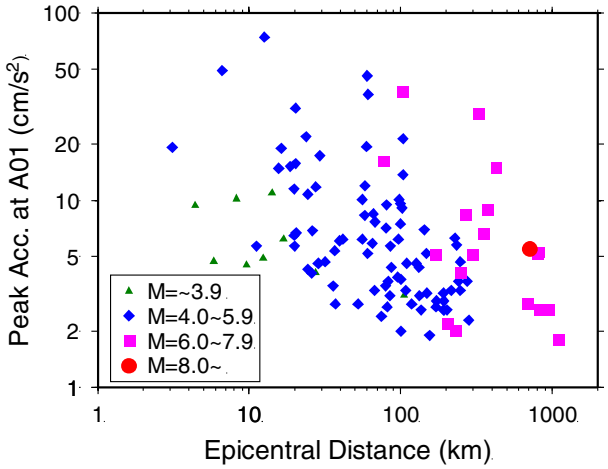

Figure 4 Relation between epicentral distances and peak accelerations at A01 (PGA)

RESULTS

Amplification of surface soil layers

A graph on the left hand in Figure 5 shows the relation between peak accelerations at A89 (89 meters below the ground) and peak acceleration ratios A01/A89. Averages of peak acceleration ratios are 1.78 and 1.83 in the N-S and E-W directions respectively. The correlation between scatterings and peak

accelerations at A89 is unclear. The graph on the right hand is relation between durations and peak acceleration ratios A01/A89. The duration is computed from U-D component at A89 using the definition of Trifunac and Brady [3]. Apparent tendency can be recognized from this graph. The peak acceleration ratios are increasing with the duration up to 40 seconds. In the range of duration more than 40 seconds, it appears that the peak acceleration ratios take constant values.

Figure 6 shows Fourier amplitude spectral ratios of acceleration records on the ground (A01) to ones at 89 meters below the ground (A89) in the horizontal directions during the earthquake of July 21, 2000 (EQ043). EQ043 gave the most intensive ground motion in terms of the JMA seismic intensity to date. The Fourier spectra are smoothed by the Parzen window with a band width of 0.1 Hz. Theoretical ratio calculated from the surface soil structure shown in Table 1 is also indicated by the dotted line in the figure. Both spectral ratios, N-S component and E-W component, have common peaks at 0.8 to 1.0 Hz, 2.2 Hz and 3 to 4 Hz. Observed results show good agreement with the theoretical ratio upon the location of peaks.

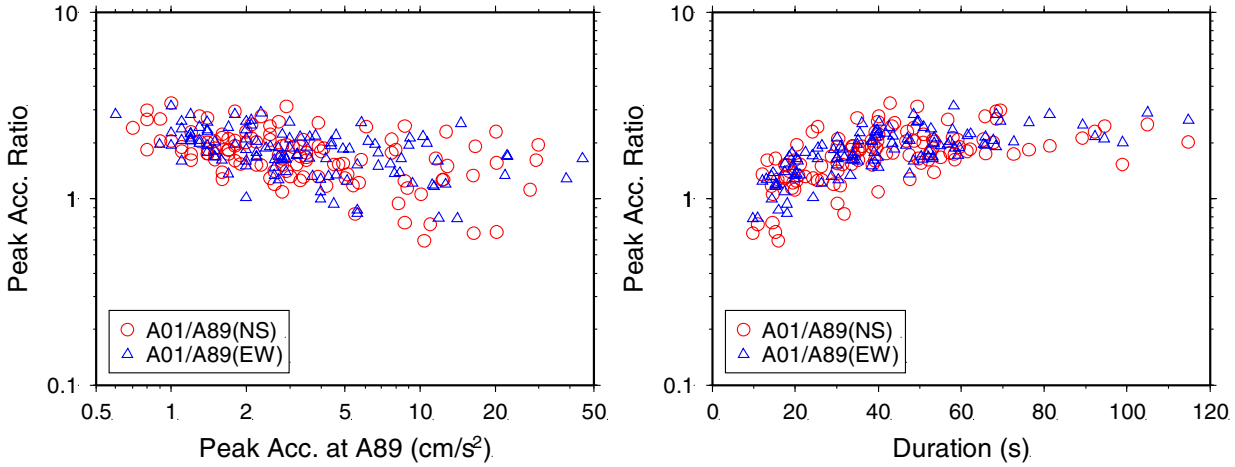

Figure 5 Relation between maximum accelerations at A89 and peak acceleration ratios A01/A89 (left), relation and between durations and peak acceleration ratios A01/A89 (right)

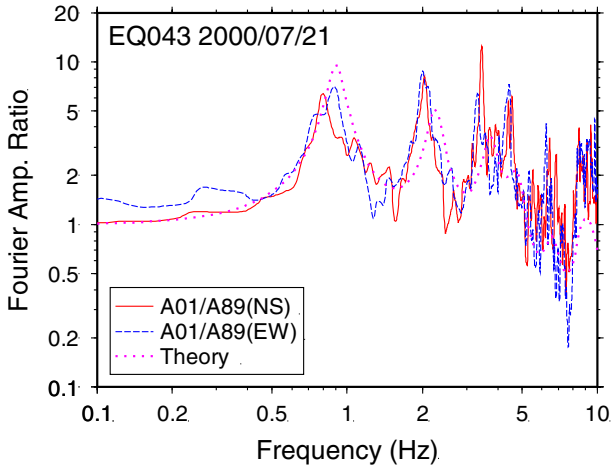

Figure 6 Fourier spectral ratios (A01/A89) in horizontal components during the earthquake of July 21, 2000

Dynamic characteristics of annex building

We discuss general dynamic characteristics of the annex building hereinafter. Figure 7 shows peak acceleration ratios BFE/A01, 8FE/BFE and 8FE/A01 in the horizontal directions. Peak accelerations at BFE are 40 to 90 % smaller than at A01. The mean values of the ratios are 0.66 and 0.61 in the N-S and E-W directions respectively. In contrast, peak acceleration ratios, 8FE/BFE and 8FE/A01, widely vary.

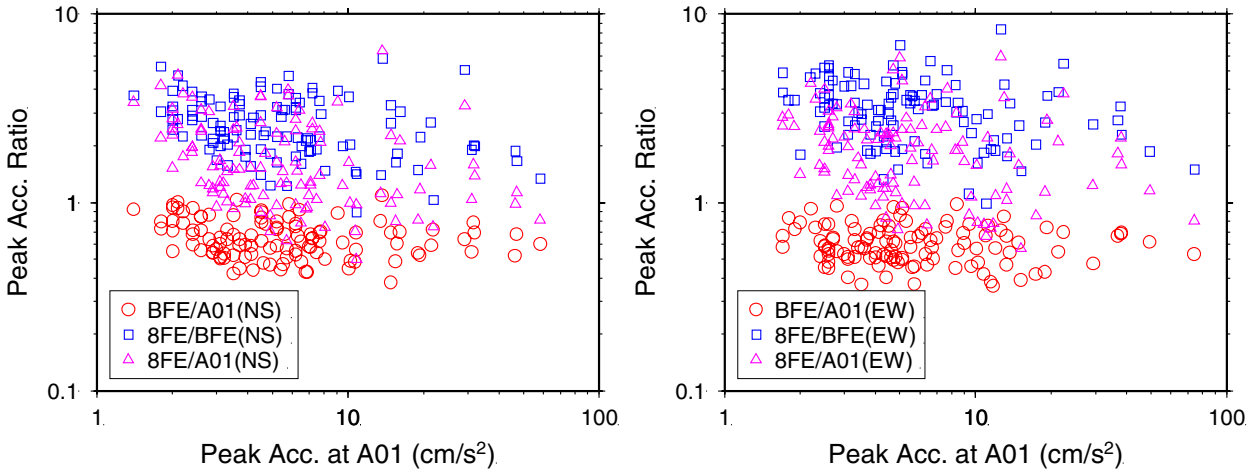

Figure 7 Peak acceleration ratios BFE/A01, 8FE/BFE and 8FE/A01 in the N-S (left) and E-W (right) components

Fourier spectral ratios BFE/A01, 8FE/A01 and 8FE/BFE for EQ043 are plotted in Figure 8. The spectral ratios 8FE/A01 and 8FE/BFE in the N-S component has clear peaks of 1.5 Hz and 2.0 Hz. The first natural frequency in the N-S direction can be estimated 1.5 Hz. The peaks at 2.0 Hz on the spectral ratios 8FE/A01 and 8FE/BFE in the N-S direction can be regarded as the torsional vibration mode for the reason below. The spectral ratio in the E-W direction also has a peak at 1.5 Hz, but doesn't have a peak of 2.0 Hz. The first natural frequency in the E-W direction is very close to the N-S direction. We note that the vibration system discussed here includes effect of the soil-structure interaction.

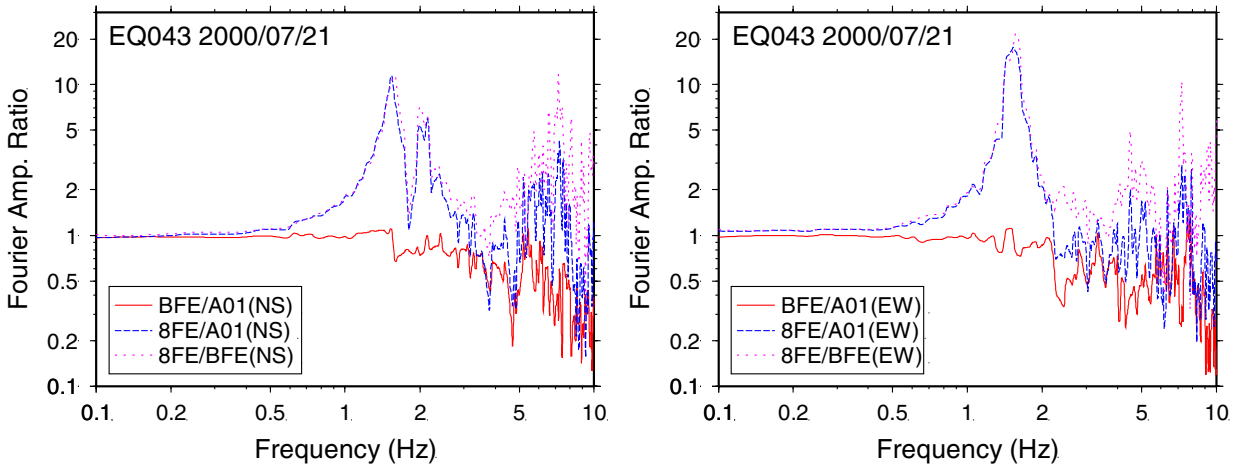

Figure 8 Fourier spectral ratios BFE/A01, 8FE/BFE and 8FE/A01 in the N-S (left) and E-W (right) components during the earthquake of July 21, 2000

Fourier spectral ratios 8FN/8FE and 8FS/8FE in the N-S direction is shown in Figure 9 in order to clarify the movement of the top floor in the horizontal plane. At frequencies 1.8 to 2.3 Hz, spectral ratios quickly

reduce and remarkable phase turning appears. This is a reason that the torsional natural frequency is estimated at 2.0 Hz.

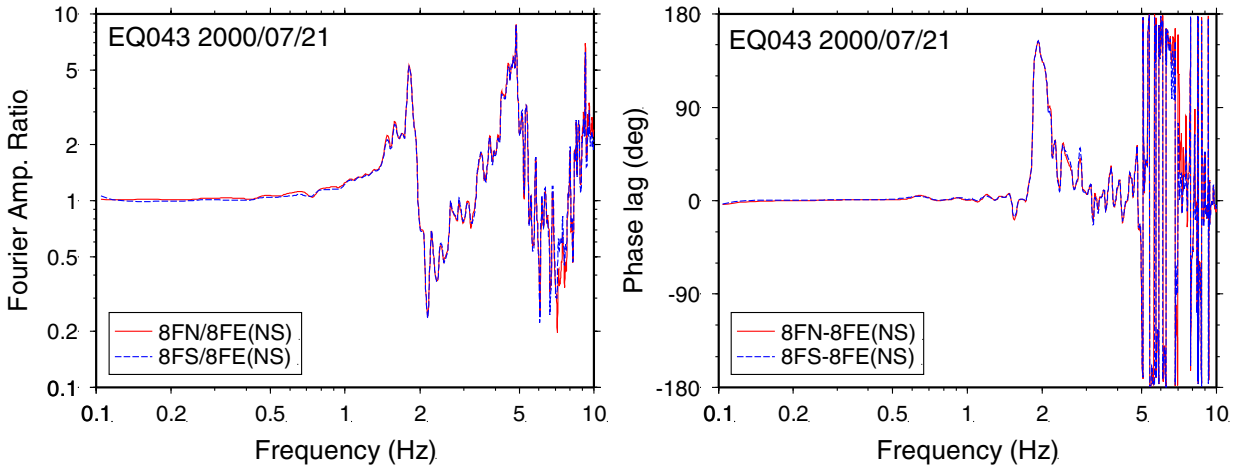

Figure 9 Fourier spectral ratios BFN/BFE and phase lag BFE-BFN during the earthquake of July 21, 2000

Effect of Soil-Structure Interaction

A simple swaying-rocking model is adopted to discuss basic properties of soil-structure interaction phenomena as shown in Figure 10. The system has two more degrees of freedom, base translation (swaying) and rotation (rocking), in addition to the building system.

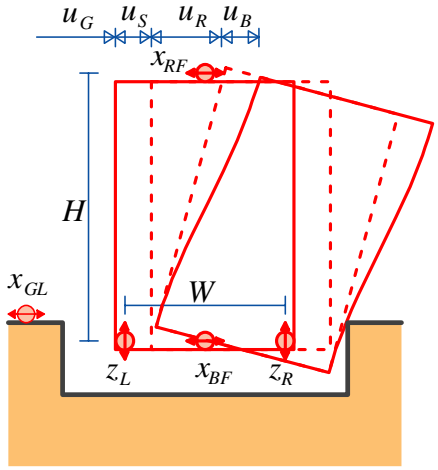

Figure 10 Swaying-rocking model

Figure 11 shows Fourier spectral ratios BFE/A01 in the N-S and E-W directions. The figure represents differences between ground earthquake motion and input motion. A dotted line indicates amplitude ratio U_{80}/U_{88}. U_{80} is the amplitudes of SH wave on the surface assuming that 8-meter topsoil is removed. U_{88} is the one of the original 88-meter soil structure model. Good agreement between observed spectral ratios and the theoretical line can be observed in the low frequency range up to 4 Hz. In the high frequency range, frequencies of peaks are consistent with theoretical ones, but heights are quite different. This may be caused by loss of input earthquake motions as a result of kinematic interaction.

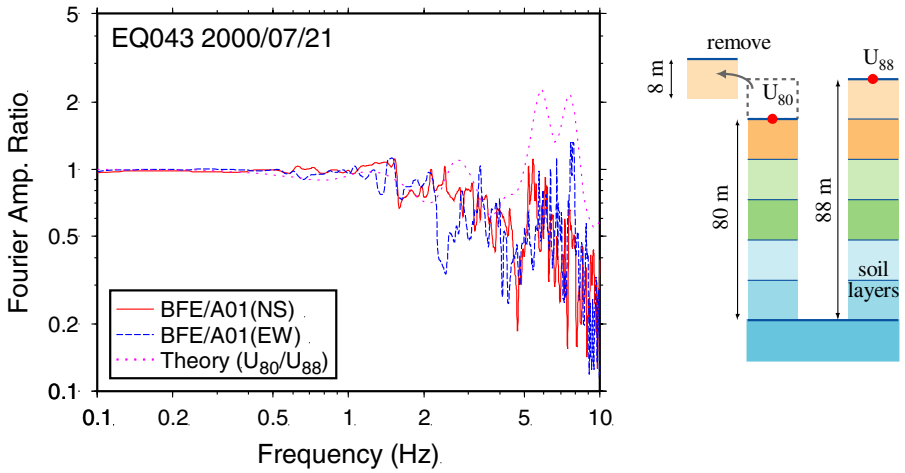

Figure 11 Fourier spectral ratios BFE/A01 in horizontal directions

Stewart and Fenves introduced system parameters for various conditions of base fixity as shown in Table 3 [4]. The "flexible base" system totally considers swaying, rocking and building deformation. The "pseudo flexible base" system takes rocking movement and building deformation into account. The "fixed base" system extracts only building deformation.

Table 3 Input and pairs of systems for various conditions of base fixity (after Stewart and Fenves [4])

System	Input	Output	Subscript
Flexible base	u_G	$u_G+u_S+u_R+u_B$	SRB
Pseudo flexible-base	u_G+u_S	$u_G+u_S+u_R+u_B$	RB
Fixed base	$u_G+u_S+u_R$	$u_G+u_S+u_R+u_B$	B

Displacement at the top floor includes the ground translation u_G, the swaying component u_S and rocking component u_R in addition to building deformation u_B. Four movements can be computed by following equations using records at five locations shown in Figure 10.

$$u_G = x_{GL} \quad (1)$$

$$u_S = x_{BF} - u_G \quad (2)$$

$$u_R = (z_L - z_R)H/W \quad (3)$$

$$u_B = x_{RF} - u_G - u_S - u_R \quad (4)$$

Figure 12 gives an example of time histories of decomposed displacements using the equations above during an actual earthquake. Displacement caused by the rocking motion has same phase with displacement by the building deformation. Ratios of the rocking displacement in the total displacement at the top floor were estimated to be 8 to 11 % [2].

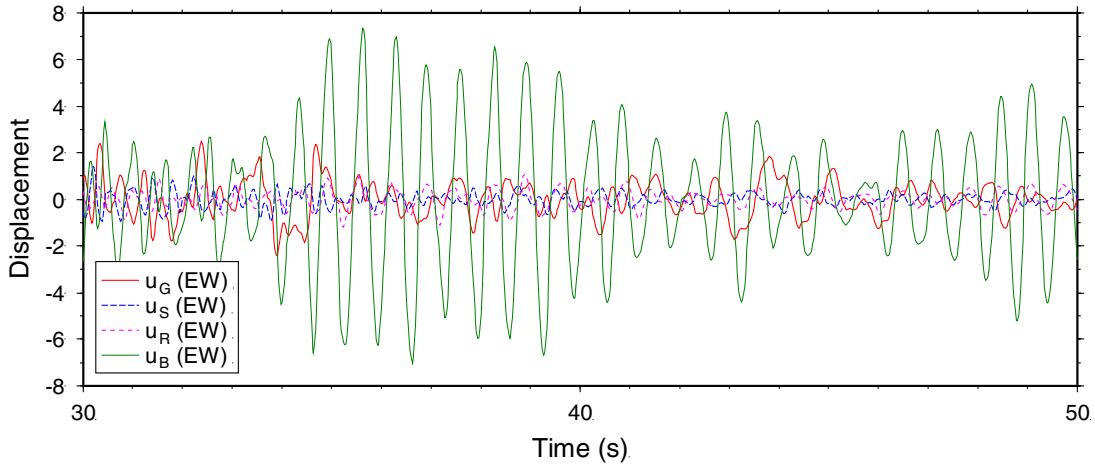

Figure 12 Displacements at the building top in the E-W direction during the earthquake of July 21, 2000

In the N-S direction, A01(NS), BFE(NS), BFN(UD) and BFS(UD) are taken as x_{GL}, x_{BF}, z_L, and z_R respectively. x_{RF} is computed from 8FS(NS)*0.8+8FE(NS)*0.2 to neglect torsional motion. In the E-W direction, A01(EW), BFE(EW), BFE(UD), BFN(UD) and 8FE(EW) are used as x_{GL}, x_{BF}, z_L, z_R and x_{RF} respectively. Transfer functions of the three systems for EQ043 are shown in Figure 13.

Terms *SRB*, *RB* and *B* indicate systems with flexible base, pseudo-flexible base and fixed base respectively. Transfer function of the system *RB* shows similar shape with the one of the system *SRB*. This means influence of swaying is not large. Transfer function of the system *B* has first peaks at higher frequencies in the both directions.

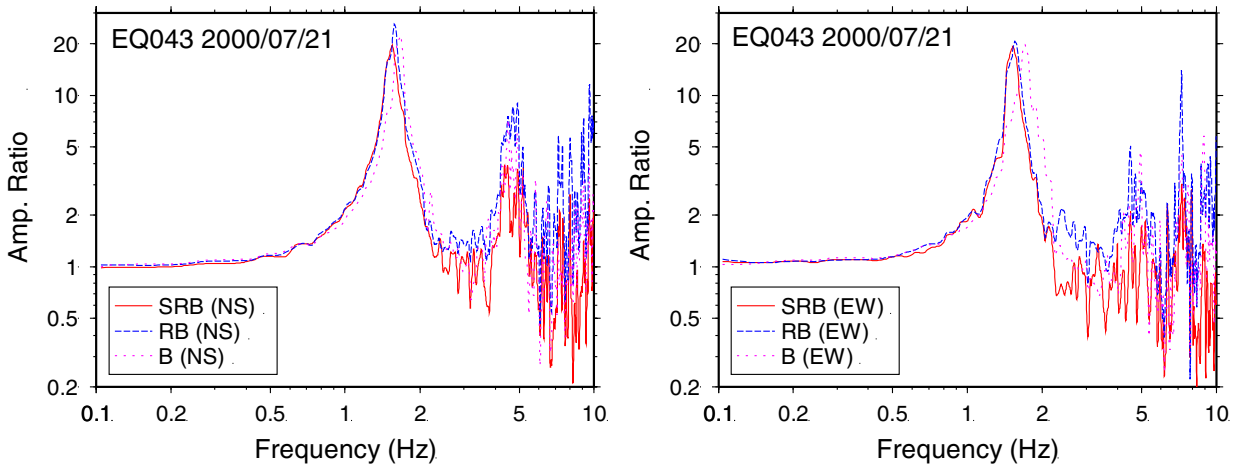

Figure 13 Transfer functions of systems with various base fixities during the earthquake of July 21, 2000

Natural frequencies (f_{SRB}, f_{RB}, f_B) and damping ratios (h_{SRB}, h_{RB}, h_B) calculated by the spectrum fitting technique of those systems are plotted in Figure 14. Subscripts *SRB*, *RB* and *B* correspond to the base fixity. Dispersion of natural frequencies and damping ratios is not small especially in the low amplitude range. Natural frequencies of the pseudo-flexible base system f_{RB} are close to ones of the flexible base system f_{SRB}. Figure 15 presents ratios of natural frequencies of the pseudo-flexible base system and the fixed base system to ones of the flexible base system (f_{RB}/f_{SRB} and f_B/f_{SRB}). Ratios in the N-S direction show

relatively small variation. The averages of ratios f_B/f_{SRB} are 1.06 and 1.11 in the N-S and E-W components respectively. The effect of the rocking motion is larger in the E-W direction.

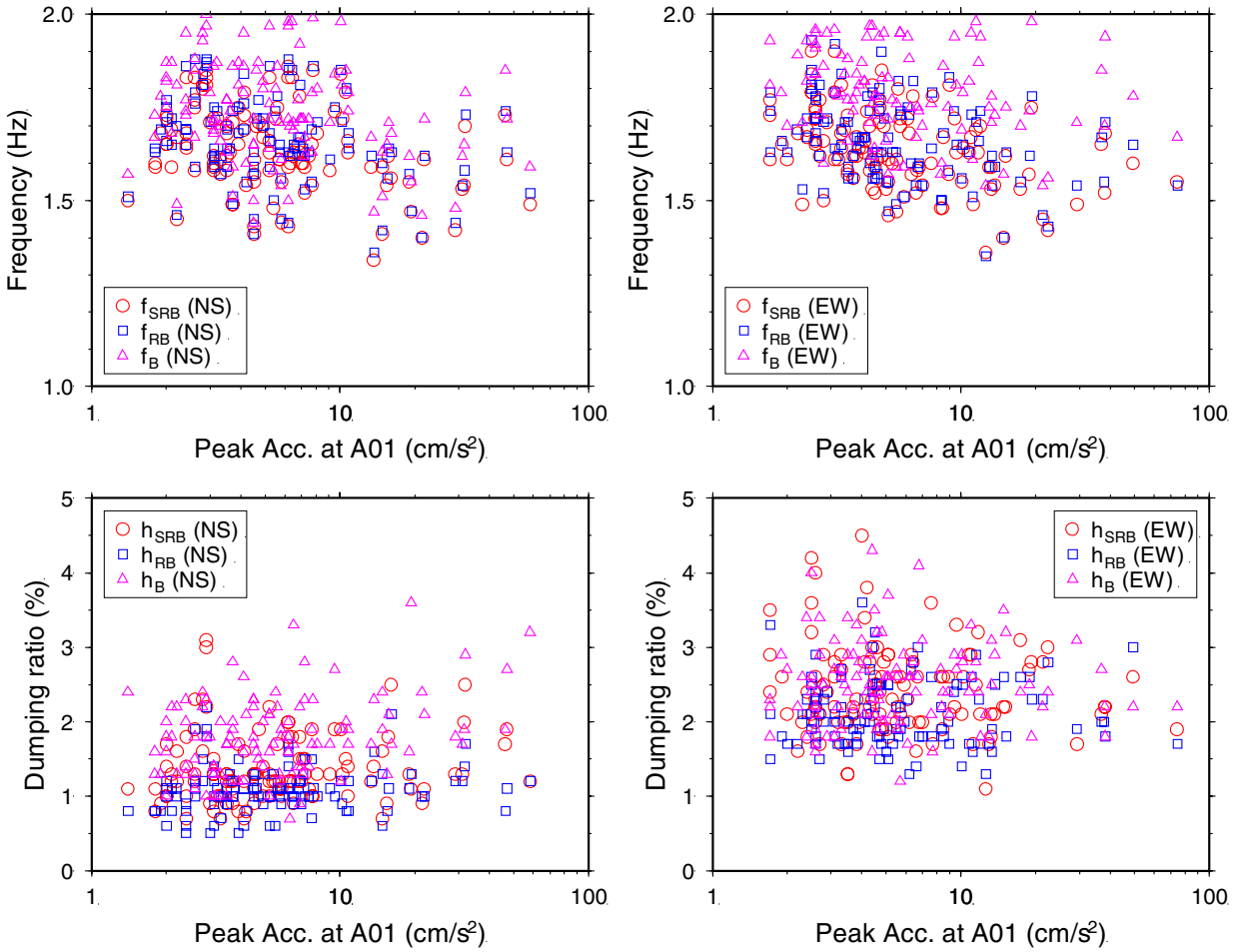

Figure 14 Natural frequencies and damping ratios of the systems with various base fixities

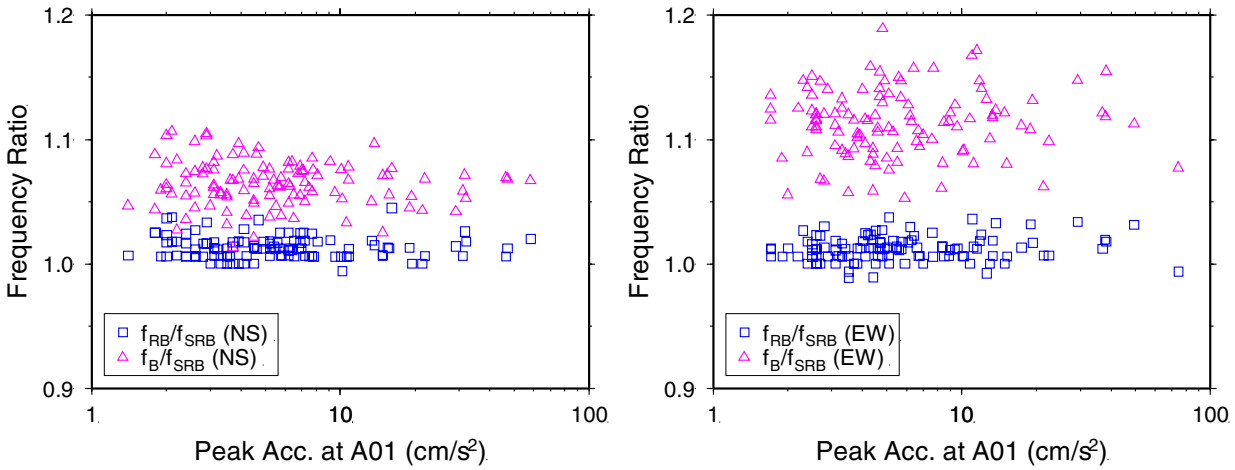

Figure 15 Ratios of natural frequencies of the pseudo-flexible base system and the fixed base system to the flexible base system

CONCLUSIONS

Building Research Institute (BRI), Japan, is conducting strong motion recording at densely instrumented buildings as a part of the strong motion network. A number of earthquake records have been obtained and analyzed. The records are useful to discuss dynamic behavior of the buildings and the grounds even though the amplitudes are small.

From records of the borehole sensors, the amplification effect of surface geology can be clearly verified. The comparison between observed records and analytical results showed good agreement.
Records of sensors in the building can explain the natural vibrations of the building. The first natural frequencies are 1.5 Hz in the N-S and E-W directions for the earthquake of July 21, 2000. The natural frequency of the torsional mode could be detected at 2.0 Hz.

The soil-structure interaction effect could be investigated using strong motion records. Natural frequencies of the flexible base system vary from 1.5 Hz to 1.8 Hz by earthquakes. The effect of the swaying is not large in general.

Amplification effects of surface geology, dynamic characteristics of a building and soil-structure interaction phenomena have been generally discussed in this paper. We intend to proceed with the study from experimental and theoretical approaches.

REFERENCES

1. I. Okawa, T. Kashima and S. Koyama, “Dense Instrumentation in BRI Buildings and Surrounding Ground”, UJNR Workshop on Soil-Structure Interaction, Menlo Park, 1998
2. T. Kashima, “Earthquake Motion Observation and SSI Characteristics of an 8-Story Building in BRI,” Second U.S.-Japan Workshop on Soil-Structure Interaction, Tsukuba, 2001
3. M. D. Trifunac and A. G. Brady (1975) “A study on the duration of strong earthquake ground motion,” Bulletin of the Seismological Society of America, Vol. 65, pp. 581-626
4. J. P. Stewart and G. L. Fenves, “System Identification for Evaluating Soil-Structure Interaction Effects in Buildings from Strong Motion Recordings,” Earthquake Engineering and Structure Dynamics 27, pp.869-885, 1998